ELSEVIER

Physica D 163 (2002) 217–235

PHYSICA D

www.elsevier.com/locate/physd

The evolution of synaptically generated waves in one- and two-dimensional domains

Remus Osan, Bard Ermentrout*

Department of Mathematics, University of Pittsburgh, Pittsburgh, PA 15260, USA

Received 2 May 2001; received in revised form 3 December 2001; accepted 13 December 2001
Communicated by C.K.R.T. Jones

Abstract

We study the onset and evolution of waves in an integrate-and-fire network of synaptically coupled neurons in one- and two-dimensional domains which are restricted to firing one spike. We determine the critical size of initial excitation of the network necessary for the onset of propagation. We also determine the ignition time. We derive an integro-differential equation for the evolution of the firing time as a function of spatial position. We use the evolution equation to understand propagation failure. We compare the behavior of the integrate-and-fire model with a biophysically based model. Finally, we show that weak heterogeneity has similarly weak effects on the firing times. © 2002 Published by Elsevier Science B.V.

Keywords: Integrate-and-fire model; Waves; Propagation failure

1. Introduction

There has been a great deal of recent theoretical interest in the propagation of waves in neural networks [1–8]. This is due in part to experimental observations in slices of pharmacologically treated tissue [9–15]. In a typical experiment, a brain slice is removed from the animal and, e.g., the inhibition is blocked by an agent such as bicuculline or picrotoxin. A local region is shocked and the resulting field potential is visualized either with multiple electrodes or with voltage-sensitive dyes. Properties such as the velocity and the initiation time can be easily measured with these techniques. Unlike the classic reaction-diffusion models, neural models involve nonlocal spatial and temporal interactions. Thus, the resulting equations are (in the continuum limit) integro-differential equations. The earliest published models for spatially organized neural networks had the form:

$$\tau \frac{\partial u(x,t)}{\partial t} = -u(x,t) + \int_D J(y-x)F(u(y,t))\,\mathrm{d}y, \tag{1}$$

where $J(x)$ is a symmetric connection function, $u(x,t)$ is the "potential" of a neural at point x in the domain D and $F(u)$ is a firing rate function. Ermentrout and McLeod [16] were the first to rigorously analyze this class of models. They showed the existence of a traveling wave front under fairly general assumptions on the functions J and F.

* Corresponding author. Tel.: +1-412-624-8324; fax: +1-412-624-8397.
E-mail address: bard@math.pitt.edu (B. Ermentrout).

0167-2789/02/$ – see front matter © 2002 Published by Elsevier Science B.V.
PII: S0167-2789(02)00347-0

These simple models arise as mean-field or averaged versions of more complicated so-called spiking models based on the biophysics of nerve membranes. More complex models with an added recovery variable have been analyzed by Amari [17], and Pinto and Ermentrout [18].

In order to get closer to the experimental questions, more realistic models for wave propagation have been introduced which incorporate voltage-gated channels and detailed synaptic transmission [13,19,20]. While some progress has been made in the analysis of these more complex models [4], most results are numerical. One simple model for a spiking neuron is the integrate-and-fire model. Each "neuron" is a linear integrator. Upon reaching a predefined threshold, V_T, the neuron emits a "spike" and the voltage is reset to $V_R < V_T$. The effect of a spike on other neurons is to turn on a current whose time dependence is often a simple exponential function and whose magnitude is a function of the distance between the two connected neurons. Thus the system is

$$\tau \frac{\partial V(x,t)}{\partial t} = -V(x,t) + g_{\text{syn}} \int_D J(|y-x|) \sum_k \alpha(t - t_k(y))\, \mathrm{d}y, \tag{2}$$

along with the reset condition such that if $V(x,t)$ crosses a threshold, V_T, it is reset to V_R. If the domain is two-dimensional, then x, y are vectors. Here $\alpha(t)$ is the time-dependent current that arises from an impulse. In the simplest models:

$$\alpha(t) = a\, \mathrm{e}^{-at} H(t),$$

where $H(t)$ is the Heaviside step function. g_{syn} is the coupling strength which we make explicit. $t_k(y)$ represents the discrete set of times that the neuron fires. That is, when $V(x,t)$ crosses V_T, the threshold for the kth time, then $V(x,t^+) = V_R$ (i.e., V is reset) and $t_k(x) = t$. Ermentrout [4], Bressloff [5], and Golomb and Ermentrout [6,7] developed methods for studying the existence of traveling waves of activity in this class of models under the assumption that *each cell only fires once*. With this assumption (which can be biologically justified by supposing strong synaptic depression or a long refractory period), it is possible to solve (2) for traveling waves and obtain an expression for the velocity, c. Indeed, a traveling wave must simply satisfying $t_1(x) \equiv t^*(x) = x/c$.

There are far fewer results on the behavior and existence of waves in two dimensions. Kistler et al. [3] studied plane waves in a two-dimensional network and also presented a stability result. This result was improved by Bressloff [21]. Milton et al. [1] and Fohlmeister et al. [22] numerically studied two-dimensional networks of integrate-and-fire models and found traveling waves of various sorts. We [23] looked at spiral waves and target waves with delayed excitation in a medium similar to the integrate-and-fire system. Clearly, an outwardly propagating target wave will asymptotically approach a plane wave which is equivalent to the one-dimensional wave problem. The differences between one- and two-dimensional waves is in the initial phases and the onset of the propagating wave. The initiation of waves in both one- and two-dimensional domains has not been looked at theoretically.

Our goal in this paper is twofold. We first study the initial-value problem in which a region is "shocked", i.e., brought to firing. We ask (i) whether this is sufficient to excite unstimulated cells; (ii) if so, how long is the delay? We then use the time of initiation as an initial condition for an evolution equation for the firing time $t^*(x)$. From this evolution equation, we can study propagation failure and other aspects of the initial formation of the traveling wave.

2. The integral form and regular waves

In this section, we convert (2) into an integral equation and reduce the question of firing times to an implicitly defined map. We explicitly compute traveling wave solutions to the integral equation.

2.1. The integral form of the integrate-and-fire model

The integrate-and-fire model equation (2) is inconvenient for the analysis of traveling waves. Under the assumption that each neuron makes a single spike, it is much easier to integrate the equations once (using $V(0) = 0$) to obtain the following integral equation for $V(x, t)$:

$$V(x, t) = g_{\text{syn}} \int_D J(y - x) A(t - t^*(y))\, \mathrm{d}y, \tag{3}$$

where

$$A(t) = \frac{1}{\tau} \int_0^t \mathrm{e}^{-(t-s)/\tau} \alpha(s)\, \mathrm{d}s.$$

If $\alpha(t) = a_1 \exp(-a_1 t) H(t)$, then

$$A(t) = \frac{a_1 a_2}{a_2 - a_1} (\mathrm{e}^{-a_1 t} - \mathrm{e}^{-a_2 t}) H(t)$$

with $a_2 = 1/\tau$, the membrane time constant. This response function is illustrated in Fig. 1 for two different choices of parameters. Since $t^*(x)$ is that time at which $V(x, t)$ first crosses threshold, this forces $V(x, t^*(x)) = V_{\text{T}}$.

Henceforth, we will work in the infinite line or plane. The firing condition for a neuron at position x in a one-dimensional network is

$$V_{\text{T}} = g_{\text{syn}} \int_{-\infty}^{\infty} \mathrm{d}y\, J(y - x) A(t^*(x) - t^*(y)). \tag{4}$$

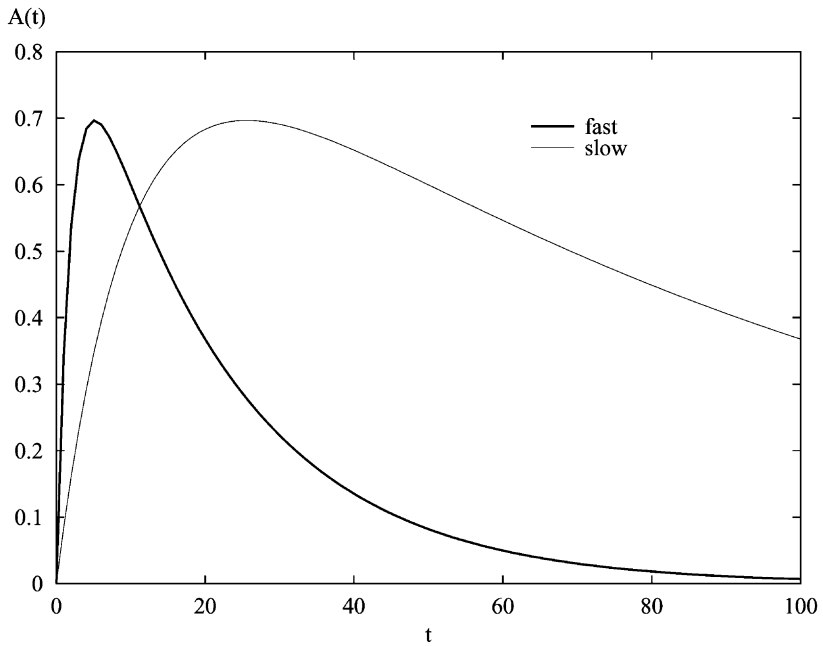

Fig. 1. Fast and slow response functions, $A(t)$ with $a_1 = 0.05$, $a_2 = 0.5$ for the fast one and $a_1 = 0.005$, $a_2 = 0.1$ for the slow one. Note the heights have been normalized here to be the same.

That is, the time at which the neuron fires, $t^*(x)$ is defined to be the first time for which $V(x,t)$ reaches threshold, V_T. If we seek radially symmetric solutions, then, the two-dimensional analogue of (4) is

$$V_T = \int_0^\infty \hat{J}(r,r')A(t^*(r) - t^*(r'))\,dr', \tag{5}$$

where

$$\hat{J}(r,r') = r' \int_0^{2\pi} J(\sqrt{r^2 + r'^2 - 2rr'\cos\theta})\,d\theta.$$

In both the one- and two-dimensional cases, the firing time is defined implicitly and thus represents a continuous, implicitly defined map. We note that a similar class of equations arises in the theory of continuous arrays of weakly coupled oscillators:

$$\Omega = \omega(x) + \int_D J(x-y)P(\theta(x) - \theta(y))\,dy,$$

where, in this case, Ω is an unknown constant, $\omega(x)$ the intrinsic frequency of each oscillator, D the domain of the network and P a periodic function.

2.2. Regular waves in the integrate-and-fire model

Before turning to the question of wave initiation, we recall the formula for the velocity for a traveling wave on the infinite one-dimensional line. For a uniform traveling wave, the firing time, $t^*(x)$ is proportional to x, i.e., $t^*(x) = x/c$, where c is the velocity. Substituting this into Eq. (4) and changing variables yields:

$$V_T = g_{syn} \int_0^\infty J(y)A\left(\frac{y}{c}\right)\,dy \equiv g_{syn}S(c), \tag{6}$$

where we have used the fact that $A(t)$ vanishes for $t < 0$. This expression gives a relationship between the velocity, c and all other parameters. The intersection of the line V_T/g_{syn} with the curve $S(c)$ gives the velocity. For example, if we choose $J(x) = \exp(-x^2)$ and

$$A(t) = \frac{a_1 a_2}{a_2 - a_1}[\exp(-a_1 t) - \exp(-a_2 t)],$$

we find that

$$S(c) = \frac{a_1 a_2}{a_2 - a_1}\frac{\sqrt{\pi}}{2}\left(e^{a_1^2/4c^2}\left(1 - \mathrm{erf}\left[\frac{a_1}{2c}\right]\right) - e^{a_2^2/4c^2}\left(1 - \mathrm{erf}\left[\frac{a_2}{2c}\right]\right)\right)$$

which is shown in Fig. 2. Note that for each sufficiently small choice of V_T/g_{syn} there is a pair of velocities. That is, if the synaptic strength is sufficiently large or the threshold is sufficiently small, then there are two traveling waves. It was shown in [5,7] that the slower of these is unstable and the fast wave is stable. Since $S(c)$ has a maximum value, the ratio V_T/g_{syn} must be sufficiently small in order for there to be traveling waves.

Ermentrout [4] used asymptotics to derive a general power-law dependence of c on the strength of the synaptic conductance, $c = O(g_{syn}^{1/p})$, where p is a positive integer depending on the shape of $\alpha(t)$. For large g_{syn} he was able to show that the same relationship holds for general conductance-based models.

The simple traveling wave *ansatz* for the one-dimensional network does not work for two dimensions since radially symmetric waves are not translation invariant. However, as $r \to \infty$ we expect the circular wave front to approach a plane wave in which case the velocity will approach the velocity given by Eq. (6). Thus, we expect that the constraints on V_T/g_{syn} for outwardly propagating waves to be the same as for one-dimensional waves.

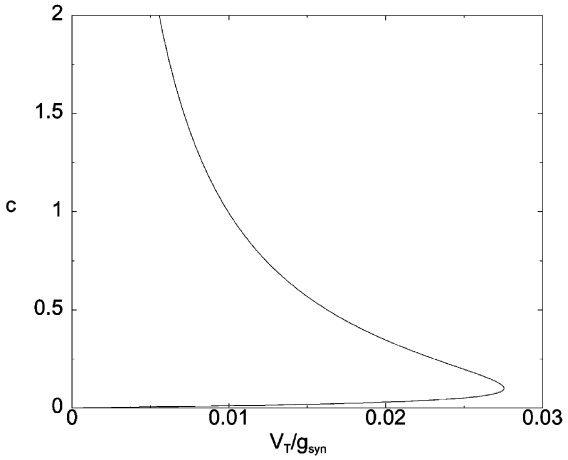

Fig. 2. The velocity of the traveling wave for a Gaussian connectivity function, $J(x) = \exp(-x^2)$ and $A(t)$ as in Fig. 1 with $a_1 = 0.05$ and $a_2 = 0.5$.

3. The initiation of the wave

In this section, we consider Eqs. (4) and (5) under conditions in which a small amount of initial tissue is excited. We then ask whether this can induce firing and if so, when does the first nonexcited cell fire? We find constraints on the parameters and the size of the excited regime which guarantee that at least one nonexcited cell in the network fires. We also determine the delay to firing of this first cell.

3.1. The initiation of the wave in the one-dimensional domain

Consider first the one-dimensional case. We suppose that $t^*(x) = -\infty$ for $x < -d$ and $t^*(x) = 0$ for $-d \le x < 0$. This states that we initially stimulate a length of tissue, d such that all neurons in this region fire synchronously. For now, we assume that the firing time is a monotonic function of their position x. Thus, $t^*(x) > t^*(y)$ if and only if $x > y$ for all nonnegative x, y. This is proven in the next section. With these considerations, we have to solve

$$\frac{V_\mathrm{T}}{g_\mathrm{syn}} = \left[\int_{-d}^{0} J(x-y)\,\mathrm{d}y\right] A(t^*(x)) + \int_0^x J(x-y)A(t^*(x)-t^*(y))\,\mathrm{d}y. \tag{7}$$

(We have used the facts that $A(0) = 0$ and $t^*(y) = 0$ for $y < 0$ to derive this from (4).) The first cell that can possibly fire is at $x = 0$ so by setting $x = 0$ in (7) we obtain

$$\frac{V_\mathrm{T}}{g_\mathrm{syn}} = A(t^*(0))\,Q(d), \tag{8}$$

where

$$Q(d) = \int_{-d}^{0} J(y)\,\mathrm{d}y = \int_0^d J(y)\,\mathrm{d}y.$$

We must solve (8) for the time of firing, $t^*(0)$. Suppose that $A(t)$ is nonnegative, vanishes at $t = 0$ and has a single maximum, A_max at $t = t_\mathrm{max}$. Suppose that $J(x) \ge 0$, symmetric, and normalized with integral 1. Then, $Q(d)$ is a

monotonically increasing function of d which approaches a value of $1/2$ as $d \to \infty$. We have the following:

1. If
$$A_{\max} > 2\frac{V_T}{g_{syn}}$$
there is a d_{crit} such that for every $d > d_{crit}$, there are two solutions to (8). We take the smaller of the two to be $t^*(0)$ as this corresponds to the potential, $V(0,t)$ *rising* past threshold. If $d < d_{crit}$ then the first cell can never fire and no wave is initiated.
2. $t^*(0)$ is a decreasing function of d. An effective connection length between neurons can be obtained by looking at how quickly $t^*(0)$ reaches a plateau as a function of the amount of stimulated tissue.
3. As d approaches d_{crit}, $t^*(0)$ approaches t_{max} which is the *maximum* time possible for initiation. For $A(t)$ as in Fig. 1
$$t_{max} = \frac{\ln(a_1/a_2)}{a_1 - a_2}.$$
The longer the synapses can persist (i.e., the smaller is a_1), the longer the possible waiting times before ignition. This is a physiologically relevant point. Pinto (Society for Neuroscience, New Orleans, 2000) reports a rather long delay before he sees the propagation of waves in a cortical slice treated with bicuculline. This indicates a possible role for some long-lasting excitatory synaptic currents. (However, see the discussion for some important differences between the integrate-and-fire model and other neural models.)
4. As $g_{syn} \to \infty$, $t^*(0) \to 0$, i.e., the stronger the synapses, the faster the initial cell fires after the stimulus.
5. The minimal value of g_{syn} required to initiate firing is less than the minimal value required to sustain a traveling wave. Thus, it is possible to initiate a wave which eventually fails. To see why this is true, we note that to initiate a wave, we must have
$$g_{syn} > \frac{V_T}{A_{\max} Q(\infty)} \equiv g^*_{init}.$$
A traveling wave with velocity c exists if
$$g_{syn} = \frac{V_T}{\int_0^\infty J(y) A(y/c)\,dy} > \frac{V_T}{A_{\max}\int_0^\infty J(y)\,dy} = g^*_{init},$$
where the last equality follows from the fact that $Q(\infty) = \int_0^\infty J(y)\,dy$.

Fig. 3 shows the dependence of t_0 on the ratio $V_T/(g_{syn}Q(d))$ for the fast alpha function shown in Fig. 1. For this particular choice, t_0 is always less than about 5 ms. As we show in the discussion, this picture looks the same for certain classes of biophysical models.

3.2. The initiation of the wave in the two-dimensional domain

The two-dimensional case is similar to the one-dimensional initiation. Suppose that we start with an initial disk of excitation with radius d. Since the connectivity is homogeneous, the radial symmetry is preserved and we will obtain radially symmetric solutions. As with the one-dimensional case, we assume that the firing time is a monotonic function of distance from initiation. Thus cells that are located at radius $r_2 > r_1$ will have firing

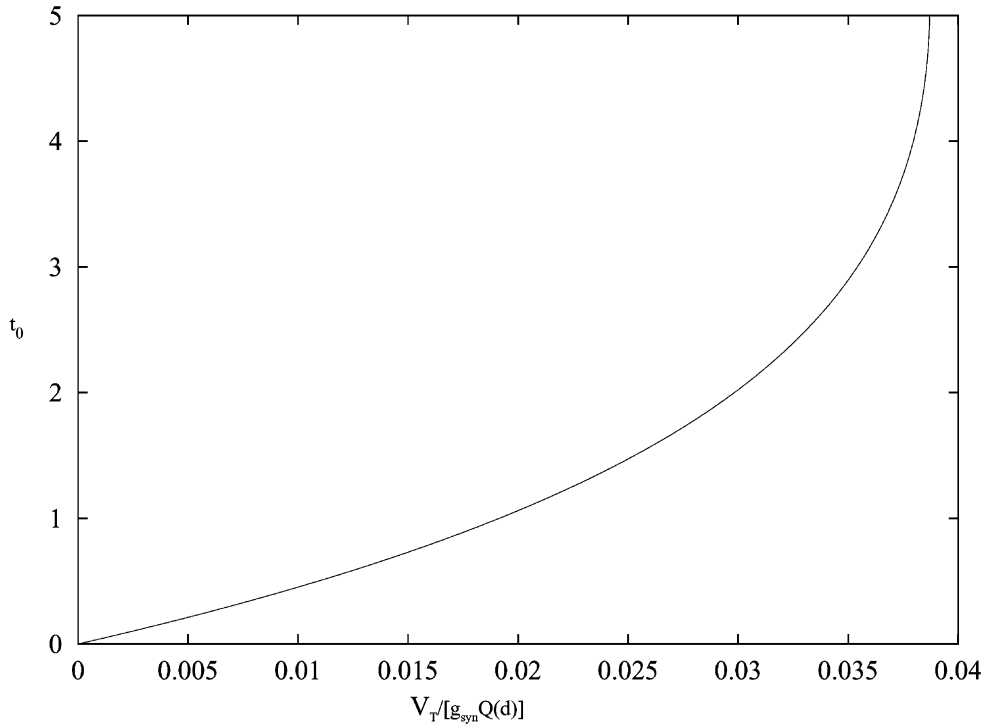

Fig. 3. The time of the initial spike as a function of threshold.

times, $t^*(r_2) > t^*(r_1)$. This implies the following implicitly defined equation:

$$\frac{V_{\mathrm{T}}}{g_{\mathrm{syn}}} = \left[\int_0^d \hat{J}(r, r')\,\mathrm{d}r'\right] A(t^*(r)) + \int_d^r \hat{J}(r, r') A(t^*(r) - t^*(r'))\,\mathrm{d}r', \tag{9}$$

defined for $r > d$. The initial firing time is found by taking the limit as $r \to d$ leading to an equation equivalent to (8):

$$\frac{V_{\mathrm{T}}}{g_{\mathrm{syn}}} = A(t^*(d))\,Q_2(d), \tag{10}$$

where

$$Q_2(d) = \int_0^d \hat{J}(d, r')\,\mathrm{d}r'.$$

$Q_2(d)$ has exactly the same properties as $Q(d)$ so that all of the statements for one-dimensional initiation also hold for two-dimensional initiation of waves. (Note that $Q_2(d) \to 1$ as $d \to \infty$, whereas $Q(d)$ tends to $1/2$. Thus $A_{\max}$ must be larger than $V_{\mathrm{T}}/g_{\mathrm{syn}}$ for the two-dimensional case.)

As an example, suppose that the coupling is a Gaussian, $J(x) = \exp(-|x|^2)/\pi$. Then

$$Q_2(d) = \frac{1}{\pi}\int_0^{2\pi} \mathrm{d}\theta \int_0^d \mathrm{d}s\, \mathrm{e}^{-[s^2+d^2+2sd\cos(\theta)]} = 2\int_0^d \mathrm{d}s\, \mathrm{e}^{-(s^2+d^2)} I_0(2sd),$$

where $I_0(x)$ is the modified Bessel function of zeroth order. Fig. 4 shows a plot of $Q_2(d)$.

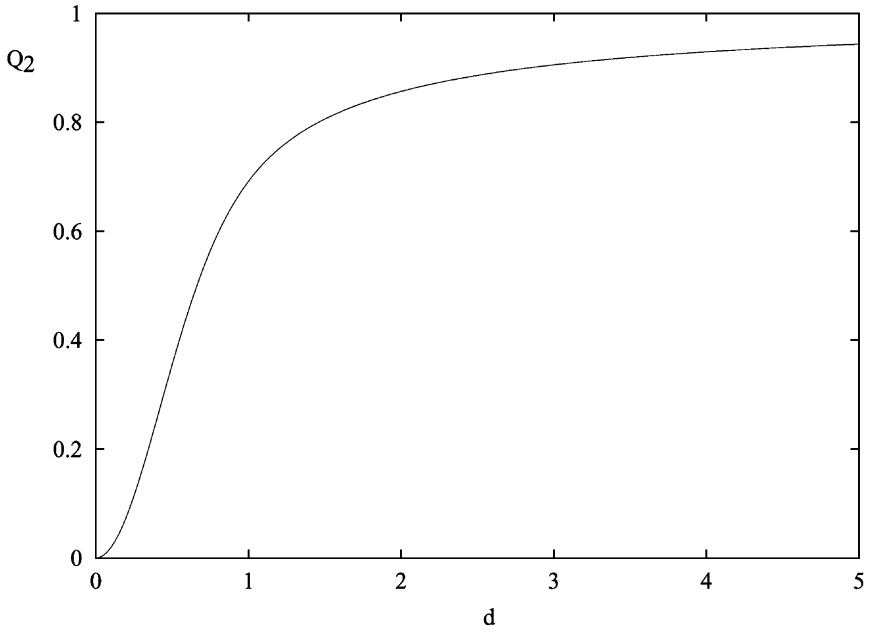

Fig. 4. The function $Q_2(d)$.

4. Computation of the firing map

Our goal in this section is to reduce the implicitly defined firing map, (3) to an evolution equation which can then be numerically integrated. In order to do this, we must first show that the firing times, $t^*(x)$ are a monotonic function of x. Thus, we first prove this and then derive a differential equation for $t^*(x)$ as a function of x. This is one of the main results in the paper; it allows us to exactly follow the time of firing rather than integrating the full equations by spatially discretizing the medium. We then discuss the qualitative behavior of the firing time equation and derive a Taylor series approximation for $t^*(x)$.

4.1. Proof of monotonicity of $t^*(x)$

Here we prove that as long as the wave persists, we must have $\mathrm{d}t^*/\mathrm{d}x > 0$. That is the cells fire monotonically in x. We will use the fact that $J(x)$ is monotonically decreasing for $x > 0$ and also the fact that $A(t)$ is nonnegative. Finally, we will also use the fact that $A'(t^*(0)) > 0$, i.e., the initiation time occurs on the rising stroke of $A(t)$. We prove monotonicity in two parts. We first show that $\mathrm{d}t^*/\mathrm{d}x > 0$ at $x = 0$. Then it follows that $t^*(x)$ must be monotonic up to some positive value of x, say b. We then show that $\partial V(x,t)/\partial x$ is negative so that the next cell to fire must be the cell at b (i.e., the maximum of $V(x,t)$ occurs at $x = b$).

We assume that at $t = 0$ all the cells for $-d < x < 0$ have been shocked and that the domain is the real line. Start with (7) and differentiate this with respect to x and evaluate it at $x = 0$ leading to

$$\frac{\mathrm{d}t^*(0)}{\mathrm{d}x} = \frac{A(t^*(0))[J(0) - J(d)]}{A'(t^*(0))Q(d)}.$$

Since J is monotonically decreasing, $A(t) > 0$ for $t > 0$, $Q(d) > 0$, and $A'(t^*(0)) > 0$ (since we choose the root on the rising branch), this implies that for sufficiently small x that $\mathrm{d}t^*/\mathrm{d}x > 0$.

On the real line, Eq. (3) becomes

$$V(x,t) = g_{\mathrm{syn}}\left[(Q(x+d) - Q(x))A(t) + \int_0^\infty J(x-y)A(t-t^*(y))\,\mathrm{d}y\right].$$

We differentiate this with respect to x to obtain

$$\frac{\partial V(x,t)}{\partial x} = g_{\mathrm{syn}}(J(x+d) - J(x))A(t) + g_{\mathrm{syn}}\int_0^\infty J'(x-y)A(t-t^*(y))\,\mathrm{d}y.$$

Since $J(x)$ is decreasing for $x > 0$ and $A(t) > 0$ for $t > 0$, it follows that $V(x,t)$ is a decreasing function of x for all t. Thus, the firing times must be monotonically increasing in x.

4.2. Evolution of the firing time

For both the one-dimensional and two-dimensional radially symmetric models, the firing times, $t^*(x)$ or $t^*(r)$ are defined implicitly as maps. Since we have proven that these times are monotonic in x, it is possible to derive an evolution equation for $t^*(x)$. Thus, in this section, we derive an integro-differential equation for the map and then solve this numerically. The numerical solution sheds insight into the mechanism by which propagation fails. We will derive the one-dimensional evolution model; the two-dimensional equation is similar in form, recall Eq. (7). We differentiate both sides with respect to x obtaining

$$0 = P(x)A'(t^*(x))\frac{\mathrm{d}t^*(x)}{\mathrm{d}x} + P'(x)A(t^*(x)) + \int_0^x J'(x-y)A(t^*(x)-t^*(y))\,\mathrm{d}y + \left[\int_0^x J(x-y)A'(t^*(x)-t^*(y))\,\mathrm{d}y\right]\frac{\mathrm{d}t^*(x)}{\mathrm{d}x},$$

where

$$P(x) = \int_{-d}^0 J(x-y)\,\mathrm{d}y,$$

where we used again $A(0) = 0$. We rearrange this into an integro-differential equation:

$$\frac{\mathrm{d}t^*(x)}{\mathrm{d}x} = -\frac{N(t^*(x),x)}{D(t^*(x),x)}, \quad 0 < x < \infty, \quad t^*(0) = t_0, \tag{11}$$

where

$$N(t^*(x),x) = P'(x)A(t^*(x)) + \int_0^x J'(x-y)A(t^*(x)-t^*(y))\,\mathrm{d}y, \tag{12}$$

$$D(t^*(x),x) = P(x)A'(t^*(x)) + \int_0^x J(x-y)A'(t^*(x)-t^*(y))\,\mathrm{d}y. \tag{13}$$

Recall that the initial condition, t_0 satisfies

$$\frac{V_{\mathrm{T}}}{g_{\mathrm{syn}}} = P(0)A(t_0) \tag{14}$$

and that we take the root, t_0 on the rising branch of $A(t)$. Both the numerator, N and the denominator D are well-defined and bounded. We point out that numerical simulations of the full spatio-temporal model and the firing-time evolution equation match quite well.

4.3. Qualitative behavior of the traveling wave

We can use Eq. (11) to qualitatively describe the evolution of the firing times. We first note that the numerator is always negative. This follows from the fact that $P'(x) < 0$, $J'(x-y) < 0$ for $y < x$ and $A(t) \geq 0$. At $x = 0$, the denominator is given by

$$D = P(0)A'(t_0)$$

and since t_0 is on the rising branch of A, i.e., $A'(t_0) > 0$, this implies that D is initially positive. Thus, from (11) $t^*(x)$ is initially increasing. Since the numerator is always negative, the evolution equation can break down only if the denominator approaches 0. When the denominator approaches 0, this means that $\mathrm{d}t^*(x)/\mathrm{d}x$ approaches infinity and implies that there is propagation failure. Thus, the wave fails to propagate if the denominator goes to zero too fast and the firing time becomes singular. If the denominator stays positive, then propagation will be sustained and solutions will approach the speed of the traveling waves constructed in Section 2. Furthermore, if there is no failure, then $t^*(x)$ is a monotone function of x as shown in the previous section. We can see why solutions approach a traveling wave by checking for self-consistency. Suppose that $t^*(x) \sim x/c$ for large x. Then

$$D(t^*(x), x) \sim \int_0^\infty J(y)A'\left(\frac{y}{c}\right)\,\mathrm{d}y$$

and

$$N(t^*(x), x) \sim \int_0^\infty J'(y)A\left(\frac{y}{c}\right)\,\mathrm{d}y.$$

Integrating N by parts reveals that

$$N(t^*(x), x) \sim -\frac{1}{c}\int_0^\infty J(y)A'\left(\frac{y}{c}\right)\,\mathrm{d}y$$

so that for large x the ratio is $-1/c$. Since $\mathrm{d}t^*/\mathrm{d}x = -N/D$, we see that for any c, $t^*(x) \sim x/c$ is an asymptotic solution. The velocity is not determined by the asymptotics of the evolution equation. Indeed, it would appear that any c will satisfy the asymptotics. Thus, the only free parameter is the initial data, t_0 so that this must determine the velocity. But, t_0 is not independent and is a function of d and all the other parameters. Thus, if we fix d and arbitrarily choose t_0 then this presumes values for the other parameters, notably $V_\mathrm{T}/g_\mathrm{syn}$ through Eq. (14). If the pair (t_0, d) is chosen to keep $V_\mathrm{T}/g_\mathrm{syn}$ constant, then the velocity will tend to the same asymptotic value. For example, if we solve (11) with an initial condition $t_{0,1}$ and then choose a different initial condition, $t_{0,2}$ we do not expect the wave to go to the same velocity as these will correspond to different thresholds. Thus, waves will travel at the same velocity if and only if the quantity, $Q(d)A(t_0)$ is constant. This is illustrated in Fig. 5 where we show the numerical solution to (11) for two choices of d and corresponding choices of t_0 such that $Q(d)A(t_0)$ is constant. Note that the wave corresponding to the larger value of d (i.e., more medium is excited) begins earlier but has the same asymptotic slope. The reciprocal of the slope is the velocity of the wave.

Conversely, fixing d and letting t_0 increase corresponds to choosing a network with increasing thresholds or decreasing coupling strength since the larger the threshold, the more delayed the onset of the first spike. Fig. 6 shows the solution to the evolution equation for different values of t_0 showing how the speed decreases (slope of curve is larger) with greater values of t_0 corresponding to larger thresholds.

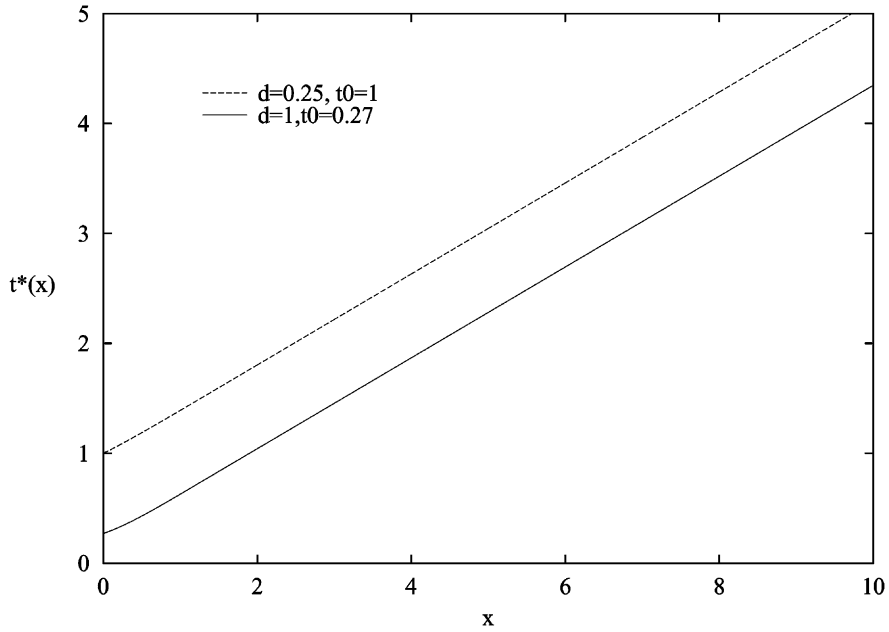

Fig. 5. Firing times for two different initial excitations and initial conditions.

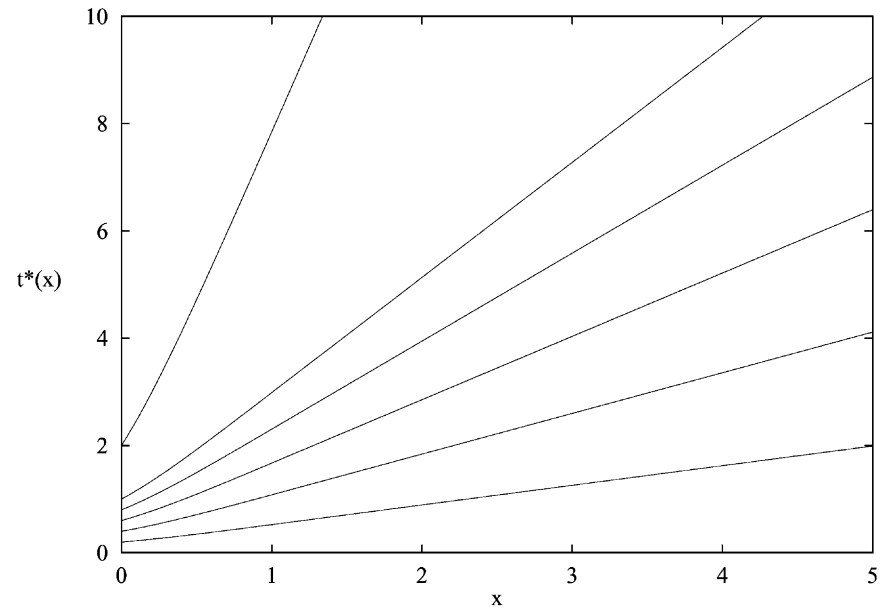

Fig. 6. Firing times for $t_0 = 2, 1, 0.8, 0.6, 0.4, 0.2$ (top to bottom) showing the slowing (steeper slope) down of the waves as the threshold increases (onset of first spike, t_0 increases).

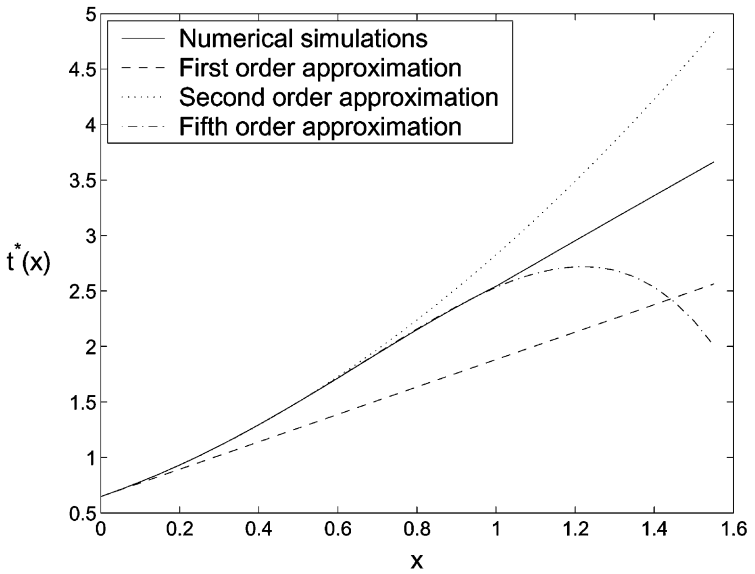

Fig. 7. Taylor expansion close to origin for a model with exponential decaying connectivity. The original excited region is responsible for generating a constant speed traveling wave.

4.4. Behavior close to origin

In Eq. (11) we derived an integro-differential equation for the evolution of the firing time as a function of spatial position. By setting $x = 0$ in Eq. (11) we can compute the inverse of the instantaneous speed of the evoked wave:

$$\frac{\mathrm{d}t^*(0)}{\mathrm{d}x} = -\frac{P'(0)A(t^*(0))}{P(0)A'(t^*(0))}. \tag{15}$$

By taking the second derivative of Eq. (7), we can compute the inverse of the instantaneous acceleration in origin:

$$\frac{\mathrm{d}^2t^*(0)}{\mathrm{d}x^2} = -\frac{P''(0)A(t^*(0)) + (2P'(0) + J(0))A'(t^*(0))(\mathrm{d}t^*(0)/\mathrm{d}x) + P(0)A''(t^*(0))(\mathrm{d}t^*(0)/\mathrm{d}x)^2}{P(0)A'(t^*(0))}. \tag{16}$$

Following the same procedure we can compute any higher order derivative of $t^*(x)$ in origin. This allows us to completely describe the behavior close to origin, obtaining a Taylor series solution to the differential equation. Clearly, as we add more terms, the quality of the approximation will improve. However, the quality of the approximation decreases quickly at large distance from origin. These features of the approximation can be observed in Fig. 7 where we show the behavior close to the origin for a wave with $A(t)$ and $J(x)$ as in previous figures.

5. How does propagation fail?

Propagation failure means that the solution to (11) cannot be continued beyond the some point x_{fail}. This happens if the denominator, D defined in Eq. (13) goes to 0. The denominator consists of two components, $D = D_1 + D_2$:

$$D_1 = P(x)A'(t^*(x)), \qquad D_2 = \int_0^x J(x-y)A'(t^*(x) - t^*(y)).$$

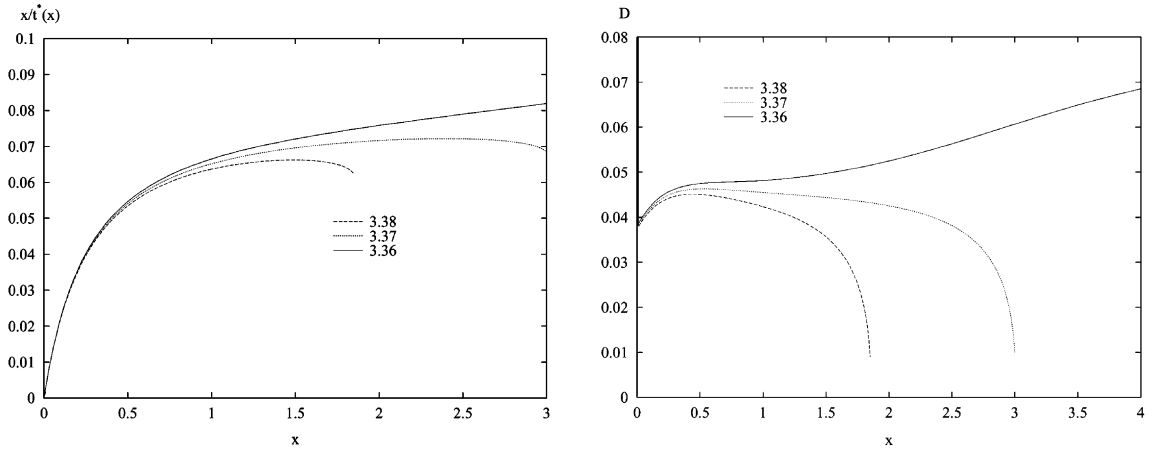

Fig. 8. (Left) The effective speed, $x/t^*(x)$ as the threshold varies. Here we parameterize the threshold by changing the time of the first spike, t_0 which is given in the legend. The larger two values lead to propagation failure. (Right) The denominator D corresponding to the three solutions in the left panel. Note the rapid downward turn as the denominator tends to 0.

Initially $D_1 > 0$ and $D_2 = 0$. For small values of x, D_1 remains positive and $D_2 > 0$. Once $t^*(x)$ crosses $t_{\max}$, D_1 changes sign and becomes negative. However, at this point, D_2 is still positive, since $t_{\max} - t^*(y) < t_{\max}$ and $J(x) > 0$. As x increases, $t^*(x)$ also increases and D_1 remains negative but gets smaller in magnitude. On the other hand, D_2, while positive may possibly start to decrease. This can happen for all x such that $t^*(x) > t_{\max} + t^*(y)$. However, if the difference, $x - y$ between these values of y are also large, then they have little contribution to the integral due to the decay properties of $J(x)$. The difference, $|x - y|$ is roughly proportional to $c|t^*(x) - t^*(y)|$. Thus, if the wave is fast (c large), then $|x - y|$ is large and the contribution of the terms such that $A'(t^*(x) - t^*(y))$ is negative are negligible as they are multiplied by a factor $J(|x - y|)$. Thus, D_2 stays larger in magnitude than D_1. Propagation failure thus occurs when the effective velocity $x/t^*(x)$ cannot get above a critical velocity.

Fig. 8 illustrates how failure occurs as the threshold is increased (or the synaptic strength is decreased). Recall that t_0 is a monotonic function of the threshold (see Fig. 3) so that increasing t_0 is equivalent to increasing V_{T}. The left panel shows the "effective speed", $x/t^*(x)$ for three values of $t_0 = t^*(0)$. It appears that for these parameters, if the initial firing time is above about 3.36, then the effective speed is too small and rather than monotonically approaching an asymptotic traveling wave, the network fails at $x = 2$. The right panel shows the rapid decline of the denominator, D which approaches the origin with infinite slope at the spatial point where failure occurs. Based on numerical simulations, it appears that failure can occur at an arbitrarily long distance from the origin. Furthermore, the same simulations indicate that failure occurs at a point x_{fail} which depends logarithmically on $t_0 - t_{0,\mathrm{crit}}$, where t_{crit} is the initial spike delay above which failure is guaranteed. A satisfactory asymptotic theory remains to be found.

In the simulations described above, we studied failure as a consequence of changing the intrinsic properties of the medium—the threshold and synaptic strength. Instead, we can hold these fixed and vary the initial size of excitation. As shown in Section 3, if the amount of medium excited is too small, then the neuron at $x = 0$ will not fire. We ask the following question: suppose the size of the initial excitation is large enough to fire the first neuron. Does it then follow that the remaining medium must fire? The answer to this is, no. This is a consequence of property 5 in Section 3.1. The ratio, $g_{\mathrm{syn}}/V_{\mathrm{T}}$ in order for a wave to initiate is always *smaller* than the ratio required to sustain a traveling wave. Thus, it is possible to initiate a wave which will eventually fail. The velocity is proportional to the ratio $g_{\mathrm{syn}}/V_{\mathrm{T}}$. If this ratio is too small, then the wave can never reach a sufficient velocity and will fail for the reasons described in the previous paragraph.

6. Discussion

We have derived equations for the initiation and propagation of synaptically generated waves in an integrate-and-fire model. The methods developed here allow us to describe how failure can occur. We have shown that it is possible to initiate a wave which will eventually fail of the synaptic strength is too low. The fact that neurons only fire once and that, once they have fired, they cannot be further influenced by the presynaptic cell makes the analysis of these integral equations considerably easier than the analogous reaction-diffusion models, i.e., the effects of one cell on another take a specified form and do not depend on the dynamics of either cell. Thus, while the interactions may be distance- and time-dependent, the resulting models are in a sense easier to analyze than are reaction-diffusion equations. The other main advantage is that we can exactly integrate the equations and reduce the existence and dynamics of the propagation to a map. Furthermore, we can reduce this implicitly defined map to a Volterra differential equation for the firing times. The ability to derive this map depends on the fact that the integrate-and-fire model can be completely solved.

The assumption of a single spike use for the integrate-and-fire model and the homogeneity of the medium are crucial for the analysis of the initiation, the transient and the asymptotic behavior of the waves. We now address these issues.

6.1. Single-spike assumption

Multiple spikes make the analysis quite difficult for at least two reasons. First, we must describe what happens to the membrane once the cell has fired. Thus, in the derivation of the integral equation (3) we must also take into consideration the resetting mechanism. For example, suppose that the membrane is reset from V_T to $V_R < V_T$. Then, a term of the form

$$\eta(t) \equiv (V_R - V_T) \exp\left(-\frac{t - t^*(x)}{\tau H(t - t^*(x))}\right)$$

must be added to the right-hand side of (3). In order to satisfy the single-spike assumption, we must check that $V(x, t)$ never again crosses threshold. If it does, then we encounter the second difficulty. We must determine the times of firing of successive spikes. These have influence on the first spikes of cells that are farther down the medium. So, we must solve for a possibly infinite family of firing times, $t_j^*(x)$. The single-spike assumption avoids this problem. By choosing V_R very negative, we can be sure that the model does not fire again. If the time constants of the synapse and the cell are short, then the result of distant cells firing decays rapidly. However, the a short membrane time constant also means that $\eta(t)$ decays rapidly as well so that there is a possibility for the neuron to again fire.

In spite of the above caveats, for some biophysical models which have slow dynamics, the recovery of the cell back to rest is long enough so that with reasonable synaptic time constants, the cell fires only one spike. Such an example is illustrated in Fig. 9. No restrictions on the number of spikes are made. The time constant of the synapse must be increased to almost 50 ms before multiple spikes naturally occur. A similar simulation of the classic Hodgkin–Huxley equations reveals that multiple spikes are very difficult to get (see Fig. 2B in [4]).

6.2. The initiation time for biophysical models

In Section 3, we showed that for the integrate-and-fire model, the initiation time of the wave is limited by the time to peak of the synaptic response function. This, in turn, is determined by the time constants of the synapse and the membrane. Thus, for the integrate-and-fire model, the delay to firing is always finite. Rinzel and Ermentrout

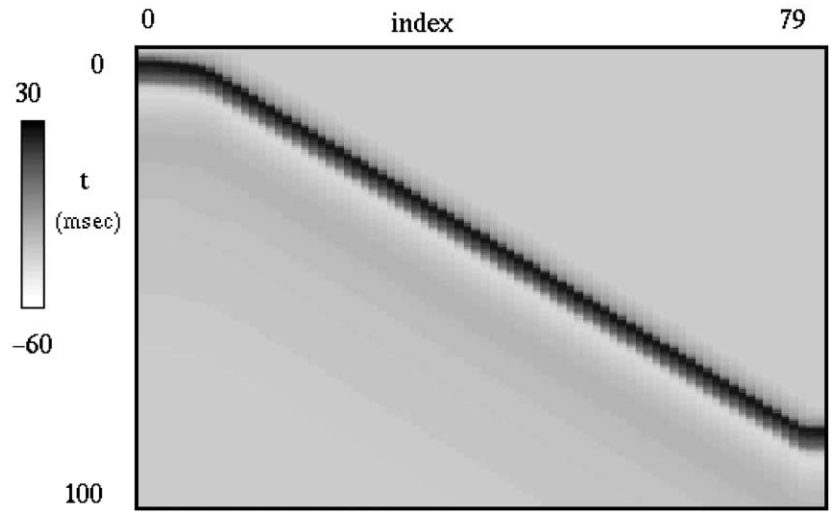

Fig. 9. Traveling wave for the Morris–Lecar model with synaptic coupling. The network has 80 cells with equal coupling to five neighbors on either side. Synapses are exponential and the threshold for firing is set to be 0 mV. Time constant of the synapse is 20 ms. Equations for the model are in Appendix A. The horizontal axis represents the cell number, the vertical is the time in milliseconds. The membrane potential is plotted in gray scale (units in millivolts). Equations are integrated using a fourth order Runge–Kutta integrator.

[24] showed that a single neuron could exhibit an arbitrarily long delay before firing. They explained this in terms of the bifurcation to oscillations that the neuron undergoes as the applied current is increased. Neurons which undergo a saddle-node bifurcation to oscillations (type I excitability) can have arbitrary latency to firing while those which undergo a sub-critical Hopf bifurcation (type II excitability) have at most finite latency. The Hodgkin–Huxley equations and the Morris–Lecar equations illustrated in Fig. 9 exhibit type II excitability. However, most cortical and hippocampal neurons for which there are models exhibit type I excitability [25].

Thus, we can ask whether the dynamics makes a difference in the onset of the wave. The voltage for the general conductance-based model satisfies

$$C\frac{\mathrm{d}V}{\mathrm{d}t} = -I_{\mathrm{ion}}(V,w) - \left(g\int_{-\infty}^{\infty} J(x-y)s(t-t^*(y))\,\mathrm{d}y\right)(V-V_{\mathrm{syn}}),$$

where $s(t)$ is the synaptic output due to a single spike. Here I_{ion} represents all the intrinsic ionic conductances and currents, and V_{syn} is the reversal potential of the synapse. As with the integrate-and-fire model, we assume that each neuron is constrained to fire just once and that $t^*(x)$ is the time of firing of the neuron at x. As above, we suppose that medium of length d is shocked and ask when the first neuron ($x = 0$) will fire. This leads to the differential equation

$$C\frac{\mathrm{d}V}{\mathrm{d}t} = -I_{\mathrm{ion}}(V,w) - gQ(d)s(t)(V-V_{\mathrm{syn}}),$$

where $Q(d)$ is as in (8) and V, w start at rest at $t = 0$. We then must solve this equation up to the point t^* at which the potential, $V(t^*)$ crosses the threshold for turning on a synapse. This is a boundary value problem with the following conditions, $V(0) = V_{\mathrm{rest}}$, $w(0) = w_{\mathrm{rest}}$ and $V(t^*) = V_{\mathrm{T}}$. By rescaling time by t^* and writing a differential equation for $s(t)$, e.g.

$$\frac{\mathrm{d}s}{\mathrm{d}t} = -\frac{s}{\tau}$$

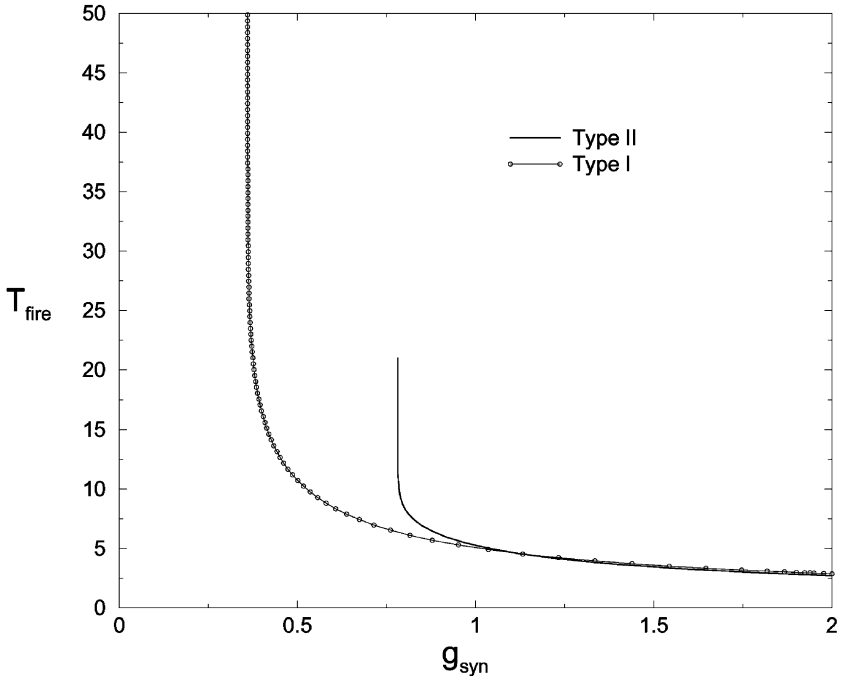

Fig. 10. Firing time as a function of g_{syn} for two different sets of parameters in the Morris–Lecar model. Type II excitability leads to a finite maximal firing time while type I excitability can have an arbitrarily long delay to firing.

with $s(0) = 1$, we can solve this boundary value problem on the interval $[0, 1]$. Fig. 10 shows the result for the Morris–Lecar model in two different parameter regimes. When the dynamics is type II (subcritical Hopf), the maximum that t^* takes is around 20 ms (commensurate with the synaptic time constant). When the dynamics is type I (saddle-node), the time to fire can be delayed arbitrarily. Thus, the integrate-and-fire results are representative of neuron model that undergoes a subcritical Hopf bifurcation.

6.3. Comparison of the propagation failure in one- and two-dimensional domains

If the initial conditions for the two-dimensional case are symmetric the evoked excitation will exhibit symmetric behavior. Propagation failure in the two-dimensional domain is qualitatively similar to the on in the one-dimensional domain.

Asymmetric initial conditions are more difficult to analyze. For example, it may be possible to have propagation failure only along one dimension. Numerical simulations could help in this regard and a systematic study remains to be done. However, results on a related model, [23] indicate that asymmetric initial data evolve into radially symmetric solutions. Thus, we expect there to be little difference in how failure occurs as we move from one-dimensional propagation to two-dimensional.

6.4. Extensions

6.4.1. Delays

Golomb and Ermentrout [6,7] showed that if there was a fixed delay between the excitation of a neuron and its neighbor, then for large enough delays the firing times no longer converge to a traveling wave. Rather, this is

unstable and the new solutions are periodically modulated. Thus, the function $A(t)$ is replaced by $A(t - t_d)$, where t_d is the delay. One should be able to use the same evolution equation to study the transient dynamics of waves in a delayed network. The numerical details are unfortunately rather complicated so that we do not attempt to solve them in this paper.

6.4.2. Heterogeneities

The waves described here are robust to small heterogeneities in the medium. For example, suppose that the coupling between neurons has the form, $J(x - y)(1 + \epsilon H(x, y))$ where H is some arbitrary function and ϵ a small parameter. The evolution equation for the firing times changes in the obvious way as does the equation for initiation. The only possible problem is that if the heterogeneity is too great, then the monotonicity of the firing times will be lost. We do not expect this to happen for small enough heterogeneities. (However, in a recent paper [26], Bressloff shows that sufficiently large heterogeneity can disrupt propagation in a firing rate model.) It is a simple perturbation calculation to assess the effects of this weak heterogeneity on steady state traveling waves. We write

$$t^*(x) = \frac{x}{c} + \epsilon\theta(x) + \cdots, \qquad c = c_0(1 + \epsilon c_1 + \cdots)$$

and substitute this into (4) obtaining

$$V_T = g_{syn}\int_{-\infty}^{\infty} J(x - y)A\left(\frac{x - y}{c_0}\right) dy,$$

$$0 = \int_{-\infty}^{\infty} J(x - y)H(x, y)A\left(\frac{x - y}{c_0}\right) dy - c_1\int_{-\infty}^{\infty} J(x - y)A'\left(\frac{x - y}{c_0}\right)\left(\frac{x - y}{c_0}\right) dy + \int_{-\infty}^{\infty} J(x - y)A'\left(\frac{x - y}{c_0}\right)\left(\frac{x - y}{c_0}\right)[\theta(x) - \theta(x)]\, dy.$$

Solving the first equation gives, c_0 the unperturbed traveling wave speed. The second equation consists of three parts. The first part is the perturbation, the second is a correction for the velocity, and the third is a convolution operator on the function $\theta(x)$. We can rewrite the second equation as

$$\int_0^{\infty} J(y)A'\left(\frac{y}{c_0}\right)\left(\frac{y}{c_0}\right)[\theta(x) - \theta(x - y)]\, dy = c_1 K - \int_0^{\infty} H(x, x - y)J(y)A\left(\frac{y}{c_0}\right) dy,$$

where

$$K = \int_0^{\infty} J(y)A'\left(\frac{y}{c_0}\right)\left(\frac{y}{c_0}\right) dy.$$

We note that $K \neq 0$ since the wave is not degenerate. The left-hand side of this equation is a linear operator which has a one-dimensional null space consisting of constant functions. Thus, we must remove the constant part of the right-hand side. This is formally done by choosing the free parameter, c_1 appropriately. Then, we can formally solve for $\theta(x)$ by taking transforms of both sides.

Thus, the main effect of heterogeneities is to perturb the velocity and to alter the firing times, but the overall wave is preserved.

Acknowledgements

Remus Osan thanks Tanase Costin for helpful discussions and suggestions. This work was funded by NSF and NIMH.

Appendix A

The Morris–Lecar equations (see [24]) are a simple three channel biophysical model for action potentials. The equations are

$$5\frac{dv}{dt} = I - 2(v+60) - 8w(v+84) - g_{Ca}m_\infty(v)(v-120),$$
$$\tau_w(v)\frac{dw}{dt} = \phi(w_\infty(v) - w), \qquad m_\infty(v) = 0.5\left(1 + \tanh\left(\frac{v+1.2}{18}\right)\right),$$
$$w_\infty(v) = 0.5\left(1 + \tanh\left(\frac{v-v_3}{v_4}\right)\right), \qquad \tau_w(v) = \frac{1}{\cosh((v-v_3)/2v_4)}.$$

The synaptic current is

$$-g_{syn}s(t)v(t)$$

and $s(t) = \exp(-t/\tau)$. Parameters for Fig. 9 are $\tau = 20$, $g_{syn} = 3$, $\phi = 0.16$, $v_3 = 2$, $v_4 = 30$, $g_{Ca} = 4.4$ and $I = 70$. Type II dynamics in Fig. 10 are identical. For type I dynamics, the parameters are $\phi = 0.25$, $v_3 = 12$, $v_4 = 17.4$ and $g_{Ca} = 4$.

References

[1] J.G. Milton, P.H. Chu, J.D. Cowan, Spiral waves in integrate-and-fire neural networks, in: S.J. Hanson, J.D. Cowan, C.L. Giles (Eds.), Advances in Neural Information Processing Systems, Vol. 5, 1993, pp. 1001–1007.
[2] D. Golomb, X.-J. Wang, J. Rinzel, Propagation of spindle waves in a thalamic slice model, J. Neurophysiol. 75 (1996) 750–769.
[3] W.M. Kistler, R. Seitz, J.L. van Hemmen, Modeling collective excitation in cortical tissues, Physica D 114 (1998) 273–295.
[4] G.B. Ermentrout, The analysis of synaptically generated traveling waves, J. Comp. Neuro. 5 (1998) 191–208.
[5] P.C. Bressloff, Synaptically generated wave propagation in excitable neural media, Phys. Rev. Lett. 82 (1999) 2979–2982.
[6] D. Golomb, G.B. Ermentrout, Continuous and lurching traveling pulses in neuronal networks with delay and spatially decaying connectivity, Proc. Natl. Acad. Sci. USA 96 (23) (1999) 13480–13485.
[7] D. Golomb, G.B. Ermentrout, Effects of delay on the type and velocity of travelling pulses in neuronal networks with spatially decaying connectivity, Network 11 (2000) 221–246.
[8] D.H. Terman, G.B. Ermentrout, A.C. Yew, Propagating activity patterns in thalamic neuronal networks, SIAM J. Appl. Math. 61 (2001) 1578–1604.
[9] R.D. Chervin, P.A. Pierce, B.W. Connors, Periodicity and directionality in the propagation of epileptiform discharges across neurocortex, J. Neurophysiol. 60 (1988) 1695–1713.
[10] R.D. Traub, J.G. Jefferys, R. Miles, Analysis of the propagation of disinhibition-induced after-discharges along the guinea-pig hippocampal slice in vitro, J. Physiol. 472 (1993) 267–287.
[11] U. Kim, T. Bal, D.A. McCormick, Spindle waves are propagating synchronized oscillations in the ferret LGNd in vitro, J. Neurophysiol. 74 (3) (1995) 1301–1323.
[12] R. Miles, R.D. Traub, R.K.S. Wong, Spread of synchronous firing in longitudinal slices from the CA3 region of the hippocampus, J. Neurophysiol. 60 (4) (1995) 1481–1496.
[13] D. Golomb, Y. Amitai, Propagating neuronal discharges in neocortical slices: computational and experimental study, J. Neurophysiol. 78 (1997) 1199–1211.
[14] R. Metherate, S.J. Cruikshank, Thalamocortical inputs trigger a propagating envelope of gamma-band activity in auditory cortex in vitro, Exp. Brain Res. 126 (2) (1999) 160–174.
[15] J.-Y. Wu, Y. Tsau, L. Guan, Propagating activation during oscillations and evoked response in neocortical slices, J. Neurosci. 19 (1999) 5005–5015.
[16] G.B. Ermentrout, J.B. McLeod, Existence and uniqueness of travelling waves for a neural network, Proc. Roy. Soc. Edinburgh A 123 (1993) 461–478.
[17] S. Amari, Dynamics of pattern formation in lateral-inhibition type neural fields, Biol. Cybern. 27 (1977) 77–87.
[18] D.J. Pinto, G.B. Ermentrout, Spatially structured activity in synaptically coupled neuronal networks. I. Traveling fronts and pulses, SIAM J. Appl. Math. 62 (2001) 206–225.

[19] R.D. Traub, R. Miles, Neuronal Networks of the Hippocampus, Cambridge University Press, Cambridge, 1991.
[20] A. Destexhe, T. Bal, D.A. McCormick, T. Sejnowski, Ionic mechanisms underlying synchronized oscillations and propagating waves in a model of ferret thalamic slices, J. Neurophysiol. 76 (3) (1996) 2049–2070.
[21] P.C. Bressloff, Traveling waves and pulses in a one-dimensional network of excitable integrate-and-fire neurons, J. Math. Biol. 40 (2000) 169–198.
[22] C. Fohlmeister, W. Gerstner, R. Ritz, J.L. van Hemmen, Spontaneous excitations in the visual cortex: stripes, spirals, rings, and collective bursts, Neural Comp. 7 (1995) 905–914.
[23] R. Osan, G.B. Ermentrout, Two-dimensional synaptically generated traveling waves in a theta-neuron neural network, Neurocomputing 38–40 (2001) 789–795.
[24] J. Rinzel, G.B. Ermentrout, Analysis of neural excitability and oscillations, in: C. Koch, I. Segev (Eds.), Methods in Neuronal Modeling: From Ions to Networks, 2nd Edition, MIT Press, Cambridge, MA, 1998, pp. 251–291.
[25] D. Hansel, G. Mato, C. Meunier, Synchrony in excitatory neural networks, Neural Comput. 7 (1995) 307–337.
[26] P.C. Bressloff, Traveling fronts and wave propagation failure in an inhomogeneous neural network, Physica D 155 (2001) 83–100.